New Physics from Flavour

M. Bona and M. Pierini
CERN, CH-1211 Geneva 23, Switzerland
M. Ciuchini, V. Lubicz, and C. Tarantino
Dipartimento di Fisica, Universitá di Roma Tre and INFN Roma III, Italy
E. Franco, G. Martinelli, and L. Silvestrini
Dipartimento di Fisica, Universitá di Roma "La Sapienza" and INFN Roma, Italy
F. Parodi and C. Schiavi
Dipartimento di Fisica, Universitá di Genova and INFN Genova, Italy
V. Sordini and A. Stocchi
Laboratoire de l'Accélérateur Linéaire, IN2P3-CNRS and Université de Paris-Sud, Orsay Cedex, France
V. Vagnoni (corresponding author)
INFN Bologna, Italy

The UT*fit* Collaboration has produced several analyses in the context of flavour physics both within and beyond the Standard Model. In this paper we present updated results for the Standard Model analysis of the Unitarity Triangle using the latest experimental and lattice QCD inputs, as well as an update of the Unitarity Triangle analysis in a scenario beyond the Standard Model. Combining all available experimental and theoretical information on $\Delta F = 2$ processes and using a model-independent parameterization, we extract the allowed New Physics contributions in the K^0, D^0, B_d, and B_s sectors. We observe a departure from the SM in the B_s sector.

1. Introduction

The UT*fit* Collaboration [1] aims to determine the coordinates $\bar{\rho}$ and $\bar{\eta}$ of the apex of the Unitarity Triangle (UT), and in general the elements of the CKM matrix [2] in the Standard Model (SM). Nowadays the SM analysis includes many experimental and theoretical results, such as predictions for several flavour observables and measurements of hadronic parameters which can be compared with the lattice QCD predictions [3]. More recently, the UT analysis has been extended beyond the SM, allowing for a model-independent determination of $\bar{\rho}$ and $\bar{\eta}$ - assuming negligible New Physics (NP) contributions to tree-level processes - and a simultaneous evaluation of the size of NP contributions to $\Delta F = 2$ amplitudes compatible with the flavour data [4, 5]. Recently, the NP analysis has been expanded to include an effective field theory study of the allowed NP contributions to $\Delta F = 2$ amplitudes. This allows to put model-independent bounds on the NP energy scale associated to flavour- and CP-violating phenomena [6].

In these proceedings we present a preliminary update of our UT analysis in the SM, including a set of fit predictions and a study of the compatibility between the fit results and some of the most interesting experimental constraints. The main difference with respect to previously published results comes from the use of updated set of lattice QCD results [7] and of some constraints ($\bar{m}_t$, α, γ, $|V_{ub}|$) updated to the latest available measurements. We also show an update of the analysis beyond the SM, with particular emphasis on NP contributions to the B_s mixing phase, where we observe a significant discrepancy with respect to the SM prediction.
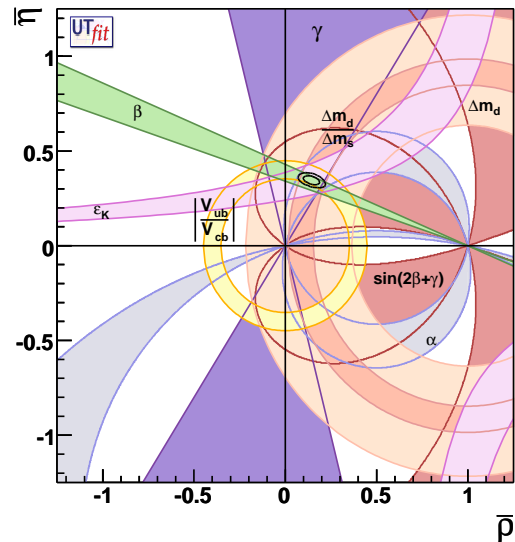

Figure 1: Result of the SM fit. The contours show the 68% and 95% probability regions selected by the fit in the $\bar{\rho}$–$\bar{\eta}$ plane. The 95% probability regions selected by the single constraints are also shown.

2. The Unitarity Triangle analysis in the Standard Model

In the UT analysis we combine the available theoretical and experimental information relevant to determine $\bar{\rho}$ and $\bar{\eta}$. To this end, we use a Bayesian approach as described in ref. [8]. The theoretical and experimental input values and errors are collected in Table I.

Table I Input parameters used in the SM UT fit. The first error corresponds to the width of a Gaussian, while the second one, whenever present, is the half width of a uniform distribution. The two distributions are then convoluted to obtain the final one. Entries marked with (†) are only indicative of the 68% probability ranges, as the full experimental likelihood has actually been used to obtain the prior distributions for these parameters. Entries without errors are considered as constants in the fit.

$\alpha_s(M_Z)$	0.119 ± 0.003
G_F	$1.16639 \cdot 10^{-5} \text{ GeV}^{-2}$
M_W	80.425 GeV
M_Z	91.1876 GeV
$\bar{m}_t(\bar{m}_t)$	$(162.8 \pm 1.3) \text{ GeV}$
$\bar{m}_b(\bar{m}_b)$	$(4.21 \pm 0.08) \text{ GeV}$
$\bar{m}_c(\bar{m}_c)$	$(1.3 \pm 0.1) \text{ GeV}$
$\bar{m}_s(2 \text{ GeV})$	$(105 \pm 15) \text{ MeV}$
M_{Bd}	5.279 GeV
M_{Bs}	5.375 GeV
τ_{B_d}	$(1.527 \pm 0.008) \text{ ps}$
τ_{B^+}	$(1.643 \pm 0.010) \text{ ps}$
τ_{B_s}	$(1.39 \pm 0.12) \text{ ps}$
$|V_{cb}|$ (exclusive)	$(3.92 \pm 0.11) \cdot 10^{-2}$
$|V_{cb}|$ (inclusive)	$(4.168 \pm 0.039 \pm 0.058) \cdot 10^{-2}$
$|V_{ub}|$ (exclusive)	$(3.5 \pm 0.4) \cdot 10^{-3}$
$|V_{ub}|$ (inclusive)	$(4.00 \pm 0.15 \pm 0.40) \cdot 10^{-3}$
ε_K	$(2.232 \pm 0.007) \cdot 10^{-3}$
M_K	497.648 MeV
f_K	160 MeV
$\hat{B}_K$	0.75 ± 0.07
Δm_d	$(0.507 \pm 0.005) \text{ ps}^{-1}$
Δm_s	$(17.77 \pm 0.12) \text{ ps}^{-1}$
$f_{B_s}\sqrt{\hat{B}_{B_s}}$	$(270 \pm 30) \text{ MeV}$
$\xi = f_{B_s}\sqrt{\hat{B}_{B_s}}/f_{B_d}\sqrt{\hat{B}_{B_d}}$	1.21 ± 0.04
λ	0.2258 ± 0.0014
$\alpha(°)$	92 ± 8 (†)
$\sin 2\beta$	0.668 ± 0.028 (†)
$\cos 2\beta$	0.88 ± 0.12 (†)
$\gamma(°)$	$(80 \pm 13) \cup (-100 \pm 13)$ (†)
$(2\beta + \gamma)(°)$	$(94 \pm 53) \cup (-90 \pm 57)$ (†)
$BR(B^+ \to \tau^+ \nu_\tau)$	$(1.12 \pm 0.45) \cdot 10^{-4}$ (†)
f_{B_d}	$(200 \pm 20) \text{ MeV}$

The results of the SM fit are shown in Table II, while the $\bar{\rho}$–$\bar{\eta}$ plane can be found in Figure 1, where the 68% and 95% probability regions are plotted together with the 95% regions selected by the single constraints. It is quite remarkable that the overall picture looks very consistent. The parameters $\bar{\rho}$ and $\bar{\eta}$ are determined in the SM with a relative errors of 14% and 4% respectively.

Within the precision of $\sim$ 5–10%, the CKM mechanism of the SM is able to describe pretty well the

Table II Results of the SM fit obtained using the experimental constraints discussed in the text. We quote the 68% [95%] probability ranges.

λ	0.2259 ± 0.0015	$[0.2228, 0.2288]$
A	0.809 ± 0.013	$[0.783, 0.835]$
$\bar{\rho}$	0.155 ± 0.022	$[0.112, 0.197]$
$\bar{\eta}$	0.342 ± 0.014	$[0.316, 0.370]$
R_b	0.377 ± 0.013	$[0.352, 0.403]$
R_t	0.911 ± 0.022	$[0.866, 0.953]$
$\alpha(°)$	92.1 ± 3.4	$[85.7, 99.0]$
$\beta(°)$	22.0 ± 0.8	$[20.5, 23.7]$
$\gamma(°)$	65.6 ± 3.3	$[58.9, 72.1]$
$|V_{cb}| \cdot 10^2$	4.125 ± 0.045	$[4.04, 4.21]$
$|V_{ub}| \cdot 10^3$	3.60 ± 0.12	$[3.37, 3.85]$
$|V_{td}| \cdot 10^3$	8.50 ± 0.21	$[8.07, 8.92]$
$|V_{td}/V_{ts}|$	0.209 ± 0.005	$[0.199, 0.219]$
$\text{Re}\lambda_t \cdot 10^3$	-0.32 ± 0.01	$[-0.34, -0.30]$
$\text{Im}\lambda_t \cdot 10^5$	13.5 ± 0.5	$[12.4, 14.6]$
$J_{CP} \cdot 10^5$	2.98 ± 0.12	$[2.75, 3.22]$
$\Delta m_s(\text{ps}^{-1})$	17.75 ± 0.15	$[17.4, 18.0]$
$\sin 2\beta_s$	0.0365 ± 0.0015	$[0.0337, 0.0394]$

Table III Fit predictions obtained without including the corresponding experimental constraints into the fit itself. We quote the 68% [95%] probability ranges.

$\alpha(°)$	92.5 ± 4.2	$[84.3, 100.5]$
$\sin 2\beta$	0.735 ± 0.034	$[0.672, 0.800]$
$\gamma(°)$	64.4 ± 3.4	$[57.6, 71.3]$
$|V_{ub}| \cdot 10^3$	3.48 ± 0.16	$[3.17, 3.80]$
$\Delta m_s(\text{ps}^{-1})$	17.0 ± 1.6	$[14.0, 20.3]$
$\sin 2\beta_s$	0.0365 ± 0.0015	$[0.0337, 0.0394]$

violation of the CP symmetry. In addition, flavour-changing CP-conserving and CP-violating processes select compatible regions in the $\bar{\rho}$–$\bar{\eta}$ plane, as predicted by the three-generation unitarity. This is illustrated on the left side of fig. 2, while on the right side we show the constraining power of the CP-violating observables (namely the UT angles) in the B_d sector only.

The results of the fit are displayed in Table II. In order to check the compatibility of the various measurements with the results of the fit, we make a comparison of the fit prediction obtained without using the observable of interest as an input and the experimental measurement. Such predictions for a subset of observables are collected in Table III.

The two most significant discrepancies between measurements and fit predictions concern $\sin 2\beta$ and the inclusive determination of $|V_{ub}|$. As can be seen in fig. 3, they are at the level of $\sim 1.5\sigma$, showing the excellent overall compatibility of the measurements with
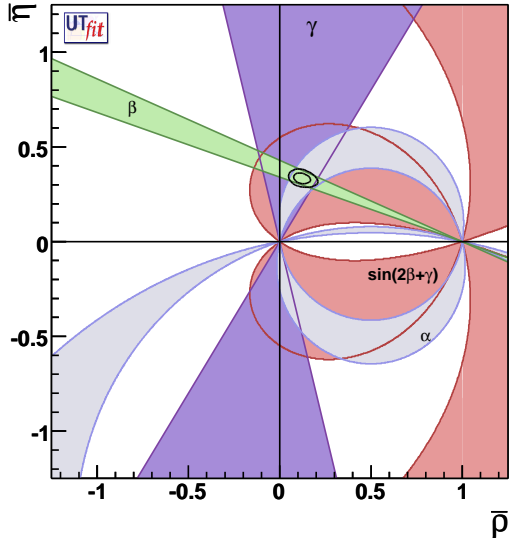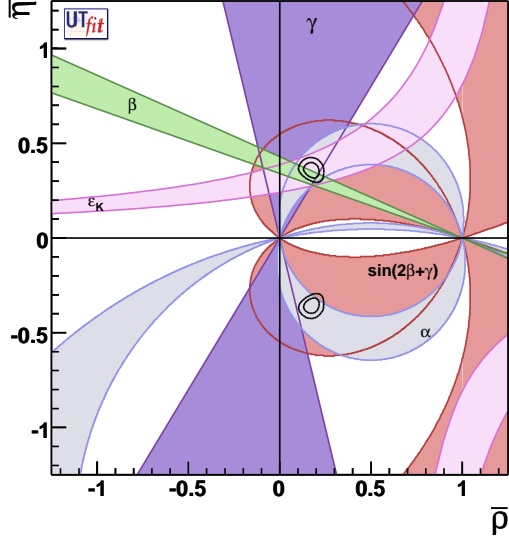
Figure 2: Constraints in the $\bar{\rho}$–$\bar{\eta}$ plane from the measurement of CP-conserving observables only (left). Constraints in the $\bar{\rho}$–$\bar{\eta}$ plane from the measurement of the angles of the UT only (right).

the SM fit (with the remarkable exception of the B_s mixing phase, as we will see in the following.

The measured value of $\sin 2\beta$ is 1.5σ smaller than the fitted one. Comparing with the recent results of ref. [9], we find that the SM fit using constraints from $|V_{ub}|$, ε_K and $\Delta m_s / \Delta m_d$ only is again 1.5σ larger than the measurement, using the input values of Table I.

3. The UT fit beyond the SM

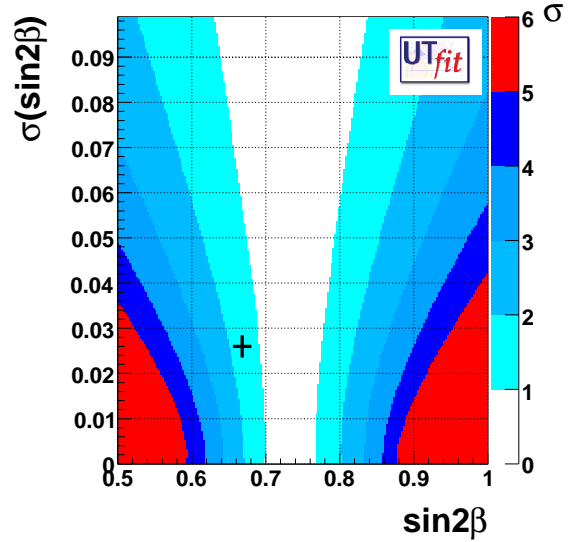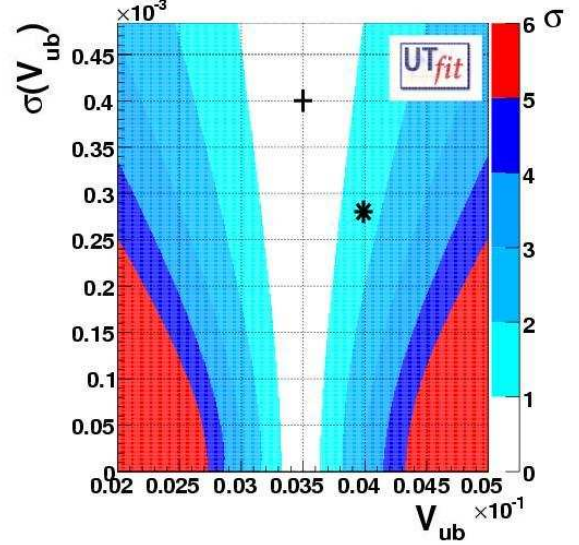Once it is established that the CKM mechanism is the main source of CP violation so far, an accurate

Figure 3: Compatibility plots for $|V_{ub}|$ (left) and $\sin 2\beta$ (right). The average value of the measurement is plotted on the horizontal axis, while its error is on the vertical one. The coloured bands delimit regions of values and errors which are less than a given number of σ from the fit result. For $|V_{ub}|$, the exclusive (denoted by "+") and inclusive (denoted by "*") measurements are shown separately.

model-independent determination of $\bar{\rho}$ and $\bar{\eta}$ is extremely important for identifying NP in the flavour sector.

The generalized UT fit, using only $\Delta F = 2$ processes and parametrizing generic NP contributions, allows for the model-independent determination of $\bar{\rho}$ and $\bar{\eta}$ under the assumptions of negligible tree-level NP contributions. Details of the method can be found in ref. [4].

A peculiar prediction of the SM is that CP violation

in B_s mixing should be very small. For this reason, the experimental observation of a sizable CP violation in B_s mixing would be an unambiguous signal of NP.

In fact, the present data give a hint of a B_s mixing phase much larger than expected in the SM, with a significance at about 3σ [5]. This result is obtained by combining all available experimental information with the method used by our collaboration for UT analyses.

We perform a model-independent analysis of NP contributions to B_s mixing using the following parameterization [6]:

$$
\begin{aligned}
C_{B_s} e^{2i\phi_{B_s}} &= \frac{A_s^{\mathrm{SM}}e^{-2i\beta_s} + A_s^{\mathrm{NP}}e^{2i(\phi_s^{\mathrm{NP}}-\beta_s)}}{A_s^{\mathrm{SM}}e^{-2i\beta_s}} = \\
&= \frac{\langle B_s|H_{\mathrm{eff}}^{\mathrm{full}}|\bar{B}_s\rangle}{\langle B_s|H_{\mathrm{eff}}^{\mathrm{SM}}|\bar{B}_s\rangle},
\end{aligned}
$$

where $H_{\mathrm{eff}}^{\mathrm{full}}$ is the effective Hamiltonian generated by both SM and NP, while $H_{\mathrm{eff}}^{\mathrm{SM}}$ only contains SM contributions. The angle β_s is defined as $\beta_s = \arg(-(V_{ts}V_{tb}^*)/(V_{cs}V_{cb}^*))$ and it equals 0.018 ± 0.001 in the SM.

We make use of the following experimental inputs: the CDF measurement of Δm_s [11], the semi-leptonic asymmetry in B_s decays A_{SL}^s [12], the di-muon charge asymmetry $A_{\mathrm{SL}}^{\mu\mu}$ from DØ [13] and CDF [14], the measurement of the B_s lifetime from flavour-specific final states [15], the two-dimensional likelihood ratio for $\Delta\Gamma_s$ and $\phi_s = 2(\beta_s - \phi_{B_s})$ from the time-dependent tagged angular analysis of $B_s \to J/\psi\phi$ decays by CDF [16] and the correlated constraints on Γ_s, $\Delta\Gamma_s$ and ϕ_s from the same analysis performed by DØ [17]. For the latter, since the complete likelihood is not available yet, we start from the results of the 7-variable fit in the free-ϕ_s case from Table I of ref. [17]. We implement the 7×7 correlation matrix and integrate over the strong phases and decay amplitudes to obtain the reduced 3×3 correlation matrix used in our analysis. In the DØ analysis, the twofold ambiguity inherent in the measurement ($\phi_s \to \pi - \phi_s$, $\Delta\Gamma_s \to -\Delta\Gamma_s$, $\cos\delta_{1,2} \to -\cos\delta_{1,2}$) for arbitrary strong phases was removed using a value for $\cos\delta_{1,2}$ derived from the BaBar analysis of $B_d \to J/\Psi K^*$ using SU(3). However, this neglects the singlet component of ϕ and, although the sign of $\cos\delta_{1,2}$ obtained using SU(3) is consistent with the factorization estimate, to be conservative we reintroduce the ambiguity in the DØ measurement, taking the errors quoted by DØ as Gaussian and duplicate the likelihood at the point obtained by applying the discrete ambiguity. Hopefully DØ will present results without assumptions on the strong phases in the future, allowing for a more straightforward combination. Finally, for the CKM parameters we perform the UT analysis in the presence of arbitrary NP as described in ref. [6], obtaining $\bar{\rho} = 0.141 \pm 0.036$ and $\bar{\eta} = 0.373 \pm 0.028$.

Table IV Fit results for NP parameters, semi-leptonic asymmetries and width differences. Whenever present, we list the two solutions due to the ambiguity of the measurements. The first line corresponds to the one closer to the SM.

Observable	68% Prob.	95% Prob.
$\phi_{B_s}[°]$	-20.3 ± 5.3	$[-30.5,-9.9]$
	-68.0 ± 4.8	$[-77.8,-58.2]$
C_{B_s}	1.00 ± 0.20	$[0.68,1.51]$
$\phi_s^{\mathrm{NP}}[°]$	-56.3 ± 8.3	$[-69.8,-36.0]$
	-79.1 ± 2.6	$[-84.0,-72.8]$
$A_s^{\mathrm{NP}}/A_s^{\mathrm{SM}}$	0.66 ± 0.28	$[0.24,1.11]$
	1.78 ± 0.03	$[1.53,2.19]$

The results of our analysis are summarized in Table IV. We see that the phase ϕ_{B_s} deviates from zero at more than 3.0σ. In Fig. 4 we present the two-dimensional 68% and 95% probability regions for the NP parameters C_{B_s} and ϕ_{B_s}, the corresponding regions for the parameters $A_s^{\mathrm{NP}}/A_s^{\mathrm{SM}}$ and ϕ_s^{NP}, and the one-dimensional distributions for NP parameters.

The solution around $\phi_{B_s} \sim -20°$ corresponds to $\phi_s^{\mathrm{NP}} \sim -56°$ and $A_s^{\mathrm{NP}}/A_s^{\mathrm{SM}} \sim 79\%$. The second solution is much more distant from the SM and it requires a dominant NP contribution ($A_s^{\mathrm{NP}}/A_s^{\mathrm{SM}} \sim 180\%$) and in this case the NP phase is very well determined.

Finally, we have tested the significance of the NP signal against different modeling of the probability density function (p.d.f.). We have explored two more methods with respect to the standard Gaussian one used by the DØ Collaboration in presenting the result: this is mainly to address the non-Gaussian tails that the experimental likelihood is showing. Firstly, we have used the 90% C.L. range for $\phi_s = [-0.06, 1.20]°$ given by DØ to estimate the standard deviation, obtaining $\phi_s = (0.57 \pm 0.38)°$ as input for the Gaussian analysis. This is conservative since the likelihood has a visibly larger half-width on the side opposite to the SM expectation (see Fig. 2 of Ref. [17]). Second, we have implemented the likelihood profiles for ϕ_s and $\Delta\Gamma_s$ given by DØ, discarding the correlations but restoring the strong phase ambiguity. The likelihood profiles include the second minimum corresponding to $\phi_s \to \phi_s + \pi$, $\Delta\Gamma \to -\Delta\Gamma$, which is disfavoured by the oscillating terms present in the tagged analysis and is discarded in the Gaussian analysis. Also this approach is conservative since each one-dimensional profile likelihood is minimized with respect to the other variables relevant for our analysis. It is remarkable that both methods give a deviation of ϕ_{B_s} from zero of $3\,\sigma$. We conclude that the combined analysis gives a stable departure from the SM, although the precise number of standard deviations depends on the procedure followed to combine presently available data.
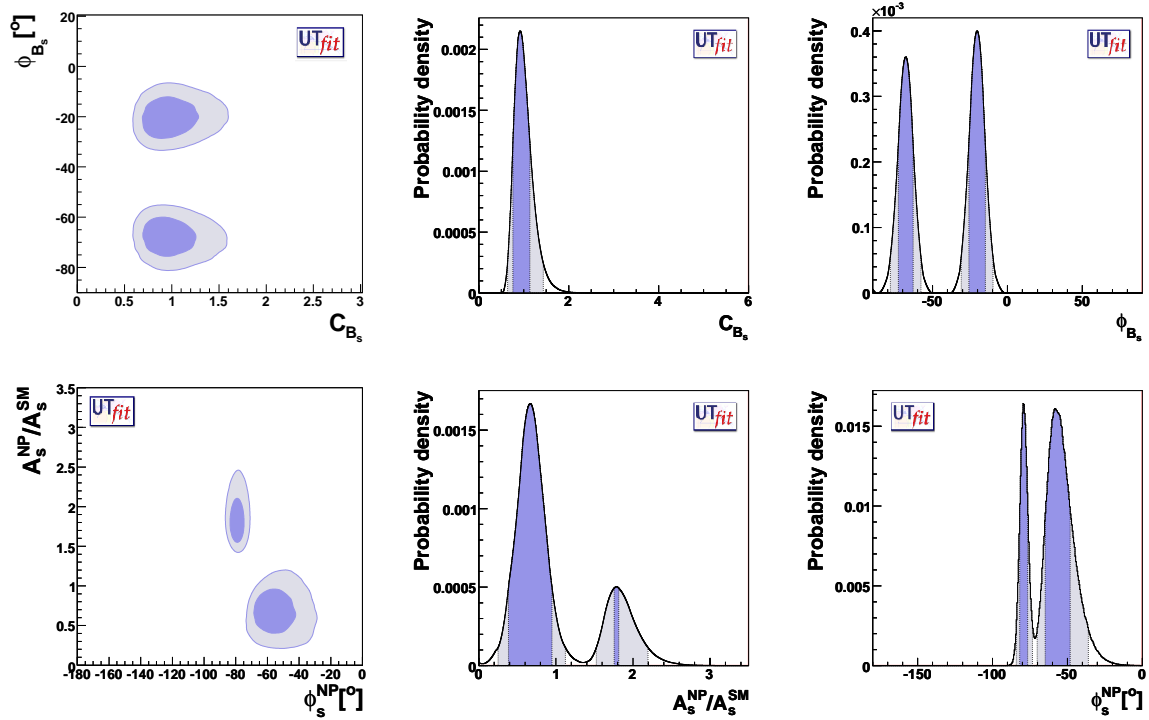
Figure 4: From left to right and from top to bottom: 68% (dark) and 95% (light) probability regions in the ϕ_{B_s}–C_{B_s} plane; p.d.f. for C_{B_s}; p.d.f. for ϕ_{B_s}; 68% and 95% probability regions in the $A_s^{\mathrm{NP}}/A_s^{\mathrm{SM}}$–$\phi_s^{\mathrm{NP}}$ plane; p.d.f. for $A_s^{\mathrm{NP}}/A_s^{\mathrm{SM}}$; p.d.f. for ϕ_s^{NP}.

References

1 UT*fit* Collaboration, http://www.utfit.org.

2 N. Cabibbo, Phys. Rev. Lett. **10** (1963) 531; M. Kobayashi and T. Maskawa, Prog. Theor. Phys. **49**, 652 (1973).

3 M. Bona *et al.* [UTfit Collaboration], JHEP **0507**, 028 (2005) [arXiv:hep-ph/0501199]; M. Bona *et al.* [UTfit Collaboration], JHEP **0610**, 081 (2006) [arXiv:hep-ph/0606167].

4 M. Bona *et al.* [UTfit Collaboration], JHEP **0603**, 080 (2006) [arXiv:hep-ph/0509219]; M. Bona *et al.* [UTfit Collaboration], Phys. Rev. Lett. **97**, 151803 (2006) [arXiv:hep-ph/0605213].

5 M. Bona *et al.* [UTfit Collaboration], arXiv:0803.0659 [hep-ph].

6 M. Bona *et al.* [UTfit Collaboration], JHEP **0803**, 049 (2008) [arXiv:0707.0636 [hep-ph]].

7 V. Lubicz and C. Tarantino, arXiv:0807.4605 [hep-lat].

8 M. Ciuchini *et al.*, JHEP **0107**, 013 (2001) [arXiv:hep-ph/0012308].

9 E. Lunghi and A. Soni, Phys. Lett. B **666**, 162 (2008) [arXiv:0803.4340 [hep-ph]].

10 M. Bona *et al.* [UTfit Collaboration], JHEP **0507**, 028 (2005); M. Bona *et al.* [UTfit Collaboration], JHEP **0610**, 081 (2006).

11 A. Abulencia *et al.* [CDF Collaboration], Phys. Rev. Lett. **97**, 242003 (2006).

12 V. M. Abazov *et al.* [D0 Collaboration], Phys. Rev. Lett. **98**, 151801 (2007).

13 V. M. Abazov *et al.* [D0 Collaboration], Phys. Rev. D **74**, 092001 (2006).

14 CDF Collaboration, CDF note 9015.

15 D. Buskulic *et al.* [ALEPH Collaboration], Phys. Lett. B **377**, 205 (1996); F. Abe *et al.* [CDF Collaboration], Phys. Rev. D **59**, 032004 (1999); P. Abreu *et al.* [DELPHI Collaboration], Eur. Phys. J. C **16**, 555 (2000); K. Ackerstaff *et al.* [OPAL Collaboration], Phys. Lett. B **426**, 161 (1998); V. M. Abazov *et al.* [D0 Collaboration], Phys. Rev. Lett. **97**, 241801 (2006); CDF Collaboration, CDF note 7386; CDF Collaboration, CDF note 7757; E. Barberio *et al.* [HFAG], arXiv:hep-ex/0603003; CDF Collaboration, CDF note 9203.

16 T. Aaltonen *et al.* [CDF Collaboration], arXiv:0712.2397 [hep-ex].

17 V. M. Abazov *et al.* [D0 Collaboration], arXiv:0802.2255 [hep-ex].